

Electronic Structure of the Abrikosov Vortex Core in Arbitrary Magnetic Fields

A. A. Golubov* and U. Hartmann†

Institute of Thin Film and Ion Technology, Kernforschungsanlage Jülich GmbH, D-52425 Jülich, Federal Republic of Germany
(Received 17 December 1993)

Using a scanning tunneling microscope we imaged Abrikosov vortex lattices in $2H\text{-NbSe}_2$. At a reduced temperature of $T/T_c=0.6$ we found a distinct decrease of the vortex-core radius with increasing magnetic field. Even at low fields $H/H_{c2}\ll 1$, the effect of vortex-vortex interactions on the spatial variation of the order parameter $\Delta(\rho)$, is clearly evident. In order to interpret the experimental results the microscopic equations of the superconducting state are solved self-consistently. A good quantitative agreement is obtained without any variational free parameters.

PACS numbers: 74.60.Ec, 61.16.Ch, 74.20.Fg, 74.50.+r

The outstanding analytical potential of scanning tunneling microscopy (STM) is due to its unique capability of providing spectroscopic information with sub-meV sensitivity at a spatial resolution of the order of angstroms. This enables one in particular to probe superconductive properties on a length scale smaller than the coherence length. The present investigations have been performed on $2H\text{-NbSe}_2$, a layered type-II compound which is relatively inert to surface contamination. The pioneering work by Hess *et al.* [1] has demonstrated that this anisotropic model superconductor is particularly well suited for the STM analysis of vortex electronic fine structures. They have shown the existence of bound states in the vortex core which are effected by vortex-vortex interactions. In the present work the influence of mutual interaction between vortices on the characteristic size of the vortex core is studied both experimentally and theoretically.

$2H\text{-NbSe}_2$ exhibits an in-plane coherence length of $\xi(0)=7.7$ nm. Most recent magnetic measurements indicate a London penetration depth of $\lambda(0)=200\text{--}250$ nm for screening by in-plane currents [2,3]. Hence, a magnetic field perpendicular to the atomic layers experiences a Ginzburg-Landau parameter of $\kappa\gg 1$ which classifies $2H\text{-NbSe}_2$ as a fairly hard type-II superconductor.

The microscope is operated in liquid helium which ensures a constant environmental reduced temperature of $T/T_c=0.6$. The surface topography of the sample is obtained in the usual way by operating the STM in the constant-current mode, typically with $I=50$ pA and $V=7$ mV at negative sample bias. Spectroscopic information is simultaneously obtained at any image point by temporarily switching the STM to an open-loop mode. Thereby the tunneling current is detected at a certain subgap voltage, where for the present investigation $V_0=0.64\Delta_0/e$ was chosen. Instrumental details can be found in Ref. [4]. While the topography of the samples usually only reveals atomic corrugation, regular Abrikosov vortex lattices become apparent from the spectroscopic data as shown in Fig. 1. For the aforementioned subgap tunneling voltage the maximum variation in tunneling current, $I_{\max}-I_{\min}$, typically amounts to about 1 pA. I_{\max} refers to the center of a vortex, while I_{\min} is

detected between two nearest neighbors. We measured the field dependence of the vortex-core radius by analyzing STM line scans along the nearest-neighbor rows of vortices for a given magnitude of the external magnetic field. The vortex-core radius is arbitrarily defined by that distance ρ_0 from the vortex center, for which the tunneling current has decreased from I_{\max} to 36% of $I_{\max}-I_{\min}$. ρ_0 values are obtained by averaging over several vortex rows, each containing a few vortices.

Since the present measurements were based on detecting variations of the tunneling current at a relatively high reduced temperature rather than on detecting variations of the differential tunneling conductivity at low reduced temperatures, $T/T_c\ll 1$, we could neither extract particular quasiparticle ground states bound to the vortex core nor a sixfold perturbation of the vortex core related to the crystal lattice [5]. Mixing of states within a few kT about the tunneling level results in completely rotationally symmetric vortex cores of roughly Gaussian shape. The STM results (see Fig. 2), however, clearly show that the vortex-core radius exhibits a pronounced shrinking due to an increasing vortex-vortex interaction under the influence of an increasing external field.

In order to understand the STM results on a firm theoretical basis, we performed calculations of the local density of states (DOS) in the Abrikosov vortex lattice at

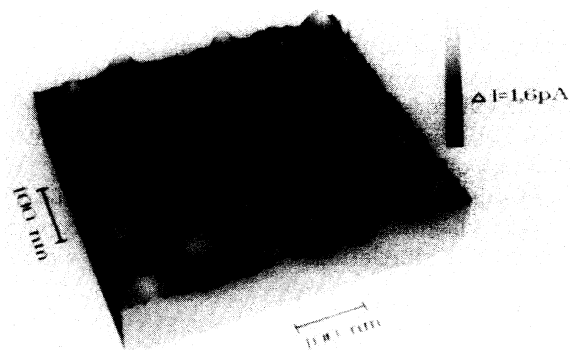


FIG. 1. Typical STM image of the vortex lattice in NbSe_2 . The external field is 0.28 T (reprinted from Ref. [4]).

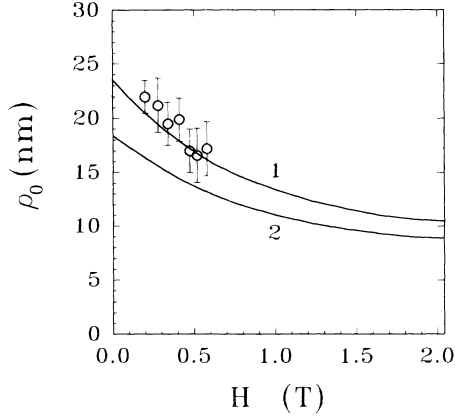


FIG. 2. Effective vortex radius for NbSe₂ as a function of magnetic field. Curve 1 represents the results of calculations for $I(\rho)$ profile; curve 2 those for $\Delta(\rho)$ profiles. The circles represent the STM data from Ref. [4]. The experimentally determined critical field values are $H_{c2}(0)=3.8$ T and $H_{c2}(0.6T_c)\cong 2.04$ T.

arbitrary magnetic fields, $0 < H < H_{c2}$. In particular, an influence of the interaction between individual vortices on order parameter, $\Delta(\rho)$, and DOS, $N(\epsilon, \rho)$, with increasing magnetic field is of interest. Earlier, the vortex-core field dependence was discussed in literature only phenomenologically in the framework of the Ginzburg-Landau (GL) equations for the order parameter [6–9]. However, the GL approach does not give a possibility to calculate the local DOS for a vortex lattice and therefore to compare the theory with STM measurements.

We restrict ourselves to a discussion of the case of relatively high T/T_c and large κ values, $\kappa \gg 1$, corresponding to the experimental situation. The calculations are done assuming dirty-limit conditions; i.e., the mean free path l is small compared to the superconducting coherence length ξ_s . In the dirty limit the equations of the microscopic theory of superconductivity are reduced to the Usadel equations [10] for the normal and anomalous Green's functions, G and F , which are valid for the whole temperature and magnetic field range:

$$\omega F - \frac{D}{2} \left[G \left(\mathbf{v} - \frac{2\pi i}{\Phi_0} \mathbf{A} \right)^2 - F \nabla^2 G \right] = \nabla G, \quad (1a)$$

$$\ln(T/T_c) + 2\pi T \sum_{\omega} (\Delta/\omega - F) = 0, \quad (1b)$$

where $D = V_F l / 3$ is the diffusion coefficient and $\omega = \pi T (2n + 1)$ is the Matsubara frequency.

We assume that the vortices form a regular lattice. In this case it is convenient to use the Wigner-Seitz method [11,12] to find the coordinate dependence of the Green's functions. In this method a hexagonal elementary unit cell of the vortex lattice is replaced by a circular one with the radius $\rho_s = (\Phi_0 / \pi H)^{1/2}$. The accuracy of this method was shown in [11,12] to be better than 0.2%. G and F depend only on the distance from the vortex core,

ρ . Introducing a new function θ by the substitution $F = \sin\theta$, $G = \cos\theta$, and transforming to cylindrical coordinates one can rewrite Eqs. (1) in the form

$$\theta'' + 1/\rho\theta' - \omega \sin\theta - Q^2(\rho) \sin\theta \cos\theta + \Delta \cos\theta = 0, \quad (2a)$$

$$\ln(T/T_c) + 2\pi T \sum_{\omega} (\Delta/\omega - \sin\theta) = 0, \quad (2b)$$

where the prime denotes differentiation with respect to ρ , and the gradient-invariant vector potential $\mathbf{Q}(\rho) = \nabla\chi - (2\pi/\Phi_0)\mathbf{A} \equiv (0, Q, 0)$ in the limit $\kappa \gg 1$ is [13]

$$Q(\rho) = 1/\rho - \rho/\rho_s^2. \quad (3)$$

Equations (2) and (3) should be supplemented with the boundary conditions at the center and the edge of the unit cell:

$$\Delta(0) = \theta(\omega, 0) = 0, \quad \Delta'(\rho_s) = \theta'(\omega, \rho_s) = 0. \quad (4)$$

Here $\Delta(\rho)$ and $\theta(\omega, \rho)$ are normalized to πT_c , the length to the coherence length $\xi_s = (D/2\pi T_c)^{1/2}$, and the magnetic field to $\Phi_0/2\pi\xi_s^2$.

In fields near H_{c2} the functions $\Delta(\rho)$ and $\theta(\omega, \rho)$ are small, which makes it possible to neglect nonlinear terms in Eqs. (2) and to obtain the solution of the linearized equations in the following form [14]:

$$\Delta(\rho) = C_0 \rho \exp(-\rho^2/2\rho_c^2), \quad (5a)$$

$$\theta(\omega, \rho) = \Delta(\rho)/(\omega + \alpha), \quad \alpha = 2/\rho_c^2 = 2\pi H_{c2}/\Phi_0. \quad (5b)$$

The constant C_0 can be found from the solution of the nonlinear equations (2), and at $T = T_c$ is equal to

$$C_0^2 = \psi_0^2(T) (1 - H/H_{c2}) / \beta_A (1 - 2e^{-1}), \quad (6)$$

where $\psi_0(T)$ is the magnitude of the bulk GL order parameter, and the parameter $\beta_A = \langle \Delta^4(\rho) \rangle / \langle \Delta^2(\rho) \rangle^2$ is 1.1576 in the Wigner-Seitz approximation [11]. Substituting Eq. (5b) into the self-consistency equation (2b), we obtain the temperature dependence of the critical cell radius $\rho_c(T)$, and the upper critical field $H_{c2}(T)$, which coincides with the Maki-de Gennes equation [15]

$$\ln(T_c/T) = \psi[1/2 + T_c \xi_s^2 / T \rho_c^2] - \psi(1/2), \quad (7)$$

where $\psi(z)$ is the digamma function. For $T \ll T_c$, expanding $\psi(1/2 + z) \cong \ln(z)$ for $z \gg 1$, and using $\psi(1/2) = -C - 2\ln 2 = -4 \ln \gamma^*$ (where $\gamma^* = e^C \cong e^{0.577} \cong 1.78$ is the Euler constant), we have from Eq. (7)

$$\Phi_0 = 4\pi \gamma^* \xi_s^2 H_{c2}(0). \quad (8)$$

For the other limit, $T \cong T_c$, Eq. (7) leads to the GL relation

$$\Phi_0 = 2\pi \xi^2(T) H_{c2}(T), \quad (9)$$

with $\xi(T) = (\pi/2) \xi_s (1 - T/T_c)^{-1/2}$. Equation (8) can be used to determine ξ_s from $H_{c2}(0)$ in order to change from a reduced length scale in units of ξ_s to a real length scale in order to compare theory and experimental data.

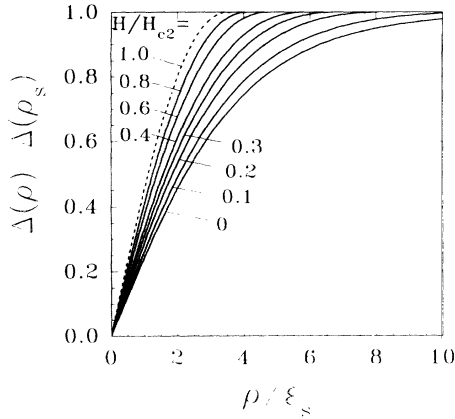


FIG. 3. Calculated spatial dependencies of the order parameter $\Delta(\rho)$ normalized to its value at the boundary of the Wigner-Seitz unit cell $\Delta(\rho_s)$, at $T=0.6T_c$ and various magnetic fields.

Using the explicit dependence of θ on the frequency ω , Eq. (5b), one can calculate the DOS by analytical continuation $\omega = -i\varepsilon$. To an accuracy of the terms of first order in $\Delta^2(\rho)$ we obtain in the limit $H \cong H_{c2}$

$$N(\varepsilon, \rho) = \text{Re}G(\varepsilon, \rho) = \text{Re}[\cos\theta(\varepsilon, \rho)] \cong 1 + \frac{\Delta^2(\rho)}{2} \frac{\varepsilon^2 - \alpha^2}{(\varepsilon^2 + \alpha^2)^2} \quad (10)$$

At arbitrary magnetic fields, $0 < H < H_{c2}$, Eqs. (2)-(4) were solved numerically. The spatial dependencies of the normalized order parameter $\Delta(\rho)/\Delta(\rho_s)$ in the vortex-core region for $T/T_c=0.6$ are shown in Fig. 3 for various H/H_{c2} values. The dashed line shows the asymptotic behavior, Eq. (5a).

The spatially resolved DOS at various distances ρ from the vortex-cell center are shown in Fig. 4 for $H/H_{c2}=0.2$. It is seen that the DOS in the vortex-core region differs qualitatively from the standard BCS curves. With increasing the distance from the vortex-cell center a peak in the DOS appears at $\varepsilon \cong \Delta_0(T)$, but the DOS remains gapless. Using these results one can calculate the tunneling current $I(\rho)$ between the superconductor with vortices and the normal conducting STM tip at various voltages and magnetic fields.

The field dependencies of resulting tunneling profiles for $eV/\Delta_0=0.64$ are shown in Fig. 5. The experimental data for $H/H_{c2}=0.2$ are also shown in order to demonstrate explicitly the fit between theory and measurements. To plot the data in absolute units we have used the experimental value of $H_{c2}(T=0)=3.8$ T for $2H\text{-NbSe}_2$. Equations (8) and (9) yield $\xi_s \cong 4.9$ nm and $\xi(0) \cong 7.7$ nm. The current at the edge of a Wigner-Seitz unit cell, I_{\min} , used in normalization, is field dependent. For $H/H_{c2}=0.2$ both theory and measurements give $I_{\min}/I_{\max} \cong 0.59$. As is seen from Fig. 5, a good fit is obtained for

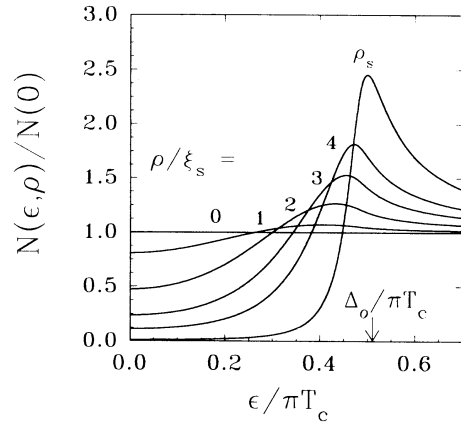


FIG. 4. Calculated spatially resolved DOS for $T=0.6T_c$ and $H/H_{c2}=0.2$ at various distances ρ from the vortex unit cell center (radius of the unit cell: $\rho_s \cong 8.16\xi_s$).

the profile curves without any variational free parameters.

Using the theoretical curves presented in Figs. 3 and 5, one can determine the effective vortex radius. First, one can define the radius as usual from the half width of $\Delta(\rho)/\Delta(\rho_s)$ according to the criterion $\Delta(\rho_{\text{eff}})/\Delta(\rho_s) = 1/\sqrt{2}$. Second, the experimentally measured effective radius is given according to the aforementioned criterion involving tunneling current variations. Both vortex radii are plotted in Fig. 2 as a function of magnetic field. The radius of an isolated vortex derived from the calculated $I(\rho)$ curve at $V_0=0.64\Delta_0/e$ and $T=0.6T_c$ is equal to $\rho \cong 23.5$ nm. The STM data are likewise shown in Fig. 2. It is seen that (1) the field dependence and the absolute values of the vortex radius calculated from the $I(\rho)$ curves are in good quantitative agreement with the data; and (2) the apparent vortex radius measured by STM is

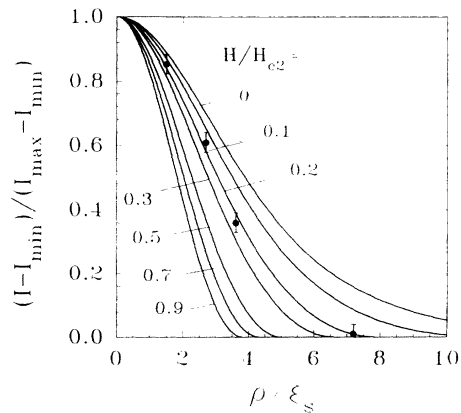


FIG. 5. Decay of the tunneling current as a function of separation from the vortex center for various magnetic fields. The circles represent STM data for $H/H_{c2}=0.2$ obtained by averaging over several vortices.

essentially larger than that defined from $\Delta(\rho)$ profiles. To demonstrate this difference more quantitatively let us define the radius ρ'_{eff} according to the same criterion as for ρ_0 , namely, $\Delta(\rho'_{\text{eff}})/\Delta(\rho_s) = 0.64$. Then it follows from Eqs. (5a) and (10) that at $H \cong H_{c2}$, $\rho'_{\text{eff}} = 0.60\xi(T)$ and $\rho_0 = 0.82\xi(T)$ for the $\Delta(\rho)$ and STM profiles, respectively; i.e., measured $I(\rho)$ scans are essentially broader than $\Delta(\rho)$ curves.

To our knowledge, the field dependence of the vortex radius has not been calculated before. The core structure was only modeled in the GL regime numerically [6,7] and by variational procedures [8,9]. In the considered high-temperature case $T = 0.6T_c$ the $\Delta(\rho)$ dependence (curve 2 in Fig. 2) given by our microscopic calculations coincides within 2% with that found from the GL equations [7]. The variational procedure by Clem [8,9] is based upon a trial order parameter function $\Delta(\rho) = \rho/(\rho^2 + \xi_v^2)^{1/2}$ that does solve the GL equations only approximately. As a result, at zero field for $\kappa \gg 1$ the parameter ξ_v is about 10% smaller than that given by exact calculations. At small fields $\xi_v(H)/\xi_v(0) = 1 - \alpha H/H_{c2}$ with $\alpha = 1$ [9], whereas our theory (curve 2 in Fig. 2) gives the result $\alpha \cong 1.13$. It is important to note, however, that the apparent vortex radius measured by tunneling can only be calculated within the microscopic theory employed in this work, because calculations of the density of states in a vortex core are beyond the framework of the GL approach. In our calculations, dirty-limit conditions were assumed. However, in the considered high-temperature region the assumption of the dirty limit does not influence the results due to the following reasons: (1) The bound states in a vortex core which exist in a clean sample [16-18] are thermally smeared out, and (2) the GL theory is valid at these temperatures. Thus the effective length scale of the spatial variation of $\Delta(\rho)$ and of $N(\epsilon, \rho)$ is given by the GL coherence length, $\xi(T)$, which is uniquely related to H_{c2} by Eq. (9) independently of the mean free path value.

In conclusion, we found an excellent agreement between the vortex effective radius measured by STM and that calculated from the Usadel equations. In order to experimentally verify the obtained relation between field magnitude and core radius for the whole range $0 < H < H_{c2}$ we are presently performing measurements in the high-field regime. This should yield some information on the DOS and vortex-radius convergence for $H \approx H_{c2}$. In spite of having performed rather fundamental investiga-

tions on a particular model superconductor we hope that the present work will contribute to a better understanding of technical materials and the behavior of superconducting devices in general.

We would like to acknowledge clarifying discussions with M. Yu. Kupriyanov (Moscow State University) and C. Heiden (University of Giessen). The samples have kindly been provided by F. Lévy (EPFL-Lausanne). The present work would not have been possible without continuous support by A. I. Braginski (KFA-Jülich).

*On leave of absence from Institute of Solid State Physics, Academy of Sciences, Chernogolovka, Moscow, Russia.

†Also at Institute of Experimental Physics, University of Saarbrücken, Saarbrücken, Federal Republic of Germany.

- [1] H. F. Hess, R. B. Robinson, R. C. Dynes, J. M. Wallis, Jr., and J. V. Waszczak, *Phys. Rev. Lett.* **62**, 214 (1989).
- [2] K. Takita and K. Masuda, *J. Low Temp. Phys.* **58**, 127 (1984).
- [3] L. P. Le, B. J. Sternlieb, W. D. Wu, Y. J. Uembura, J. W. Brill, and H. Drulis, *Physica (Amsterdam)* **185-189C**, 2715 (1991).
- [4] U. Hartmann, T. Drechsler, and C. Heiden, *SPIE Conf. Proc.* **1855**, 140 (1993).
- [5] H. F. Hess, R. B. Robinson, and J. V. Waszczak, *Phys. Rev. Lett.* **64**, 2711 (1990).
- [6] A. L. Fetter and P. C. Hohenberg, in *Superconductivity*, edited by R. D. Parks (Dekker, New York, 1969), p. 817.
- [7] M. Yu. Kupriyanov and K. K. Likharev, *JETP Lett.* **15**, 247 (1972).
- [8] J. R. Clem, *J. Low Temp. Phys.* **18**, 427 (1975).
- [9] Z. Hao, J. R. Clem, M. W. McElfresh, L. Civale, A. P. Malozemoff, and F. Holtzberg, *Phys. Rev. B* **43**, 7609 (1991).
- [10] K. Usadel, *Phys. Rev. Lett.* **25**, 560 (1970).
- [11] D. Ihle, *Phys. Status Solidi (b)* **47**, 423 (1971).
- [12] R. Watts-Tobin, L. Kramer, and W. Pesch, *J. Low Temp. Phys.* **17**, 71 (1974).
- [13] M. Yu. Kupriyanov and K. K. Likharev, *Sov. Phys. JETP* **41**, 755 (1976).
- [14] A. A. Golubov and M. Yu. Kupriyanov, *J. Low Temp. Phys.* **70**, 83 (1988).
- [15] D. Saint-James, G. Sarma, and E. J. Thomas, *Type II Superconductivity* (Pergamon, Braunschweig, 1969).
- [16] U. Klein, *Phys. Rev. B* **41**, 4819 (1990).
- [17] F. Gygi and M. Schluter, *Phys. Rev. B* **43**, 7609 (1991).
- [18] B. Pottinger and U. Klein, *Phys. Rev. Lett.* **70**, 2806 (1993).

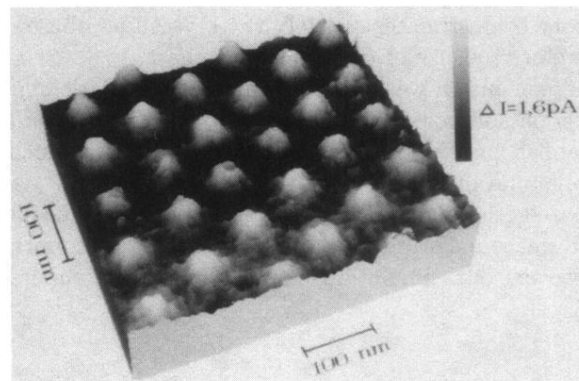


FIG. 1. Typical STM image of the vortex lattice in NbSe₂. The external field is 0.28 T (reprinted from Ref. [4]).